

Pharmacokinetics and Metabolism of 2-Aminothiazoles with Antiprion Activity in Mice

B. Michael Silber • Satish Rao • Kimberly L. Fife • Alejandra Gallardo-Godoy • Adam R. Renslo • Deepak K. Dalvie • Kurt Giles • Yevgeniy Freyman • Manuel Elepano • Joel R. Gevertz • Zhe Li • Matthew P. Jacobson • Yong Huang • Leslie Z. Benet • Stanley B. Prusiner

Received: 18 April 2012 / Accepted: 11 October 2012 / Published online: 16 February 2013
© Springer Science+Business Media New York 2013

ABSTRACT

Purpose To discover drugs lowering PrP^{Sc} in prion-infected cultured neuronal cells that achieve high concentrations in brain to test in mouse models of prion disease and then treat people with these fatal diseases.

Methods We tested 2-AMT analogs for EC₅₀ and PK after a 40 mg/kg single dose and 40–210 mg/kg/day doses for 3 days. We calculated plasma and brain AUC, ratio of AUC/EC₅₀ after dosing. We reasoned that compounds with high AUC/EC₅₀ ratios should be good candidates going forward.

Results We evaluated 27 2-AMTs in single-dose and 10 in 3-day PK studies, of which IND24 and IND81 were selected for testing in mouse models of prion disease. They had high concentrations in brain after oral dosing. Absolute bioavailability ranged from 27–40%. AUC/EC₅₀ ratios after 3 days were >100 (total) and 48–113 (unbound). Stability in liver microsomes ranged from 30–>60 min. Ring hydroxylated metabolites were observed in microsomes. Neither was a substrate for the MDRI transporter.

Conclusions IND24 and IND81 are active *in vitro* and show high AUC/EC₅₀ ratios (total and unbound) in plasma and brain. These will be evaluated in mouse models of prion disease.

Electronic supplementary material The online version of this article (doi:10.1007/s11095-012-0912-4) contains supplementary material, which is available to authorized users.

KEY WORDS antiprion drugs • drug discovery • IND24 • IND81 • prion disease

ABBREVIATIONS

2-AMT	2-aminothiazole scaffold
AUC	area under the drug concentration time curve
C _{3-day}	drug concentration after 3 days of dosing
CJD	Creutzfeldt-Jakob disease
Cl	clearance (total, intrinsic, hepatic, or otherwise)
C _{max}	maximum drug concentration
dpi	days postinoculation with prions
EC ₅₀	potency; drug concentration producing 50% of the maximal effect
FaSSIF	fasted-state simulated intestinal fluid
HTS	high-throughput screening
IV	intravenous
MDCK-MDRI	Madin Darby canine kidney cells transfected with MDRI gene

B. M. Silber • S. Rao • K. L. Fife • K. Giles • Y. Freyman • M. Elepano • J. R. Gevertz • Z. Li • S. B. Prusiner
Institute for Neurodegenerative Diseases, University of California
San Francisco, California, USA

B. M. Silber • S. Rao • K. Giles • J. R. Gevertz • Z. Li • S. B. Prusiner
Department of Neurology, University of California
San Francisco, California, USA

B. M. Silber • K. L. Fife • Z. Li • Y. Huang • L. Z. Benet
Department of Bioengineering and Therapeutic Sciences
University of California
San Francisco, California, USA

A. Gallardo-Godoy • A. R. Renslo
Small Molecule Discovery Center, University of California
San Francisco, California, USA

A. R. Renslo • M. P. Jacobson
Department of Pharmaceutical Chemistry, University of California
San Francisco, California, USA

D. K. Dalvie
Pfizer Global Research & Development
La Jolla, California, USA

S. B. Prusiner (✉)
675 Nelson Rising Ln, Room 318
San Francisco, California 94143-0518, USA
e-mail: stanley@ind.ucsf.edu

MDR1	multidrug resistance protein 1, ATP-binding cassette sub-family B member 1
MIC	minimum inhibitory concentration
P-gp	p-glycoprotein
PK	pharmacokinetics
PO	oral
PrP ^C	benign normally occurring prion protein on cell surface or inside cell
PrP ^{Sc}	abnormal, misfolded, pathogenic form of PrP ^C
RML	Rocky Mountain Laboratory
SAR	structure-activity relationship
ScN2a-cl3	scrapie (RML)-infected neuroblastoma cells that overexpress PrP ^C
V	volume of distribution (steady-state or otherwise)

INTRODUCTION

Among the neurodegenerative disorders, one group of diseases is caused by an alternatively folded prion protein (PrP) isoform (1–3). PrP is converted from its cellular isoform, PrP^C, to an alternative conformer, PrP^{Sc}, which accumulates and causes CNS dysfunction. The conversion of PrP^C into PrP^{Sc} can occur spontaneously, be induced by an autosomal dominant mutation of the PrP gene or result from exposure to exogenous PrP^{Sc} (4). The infectious nature of prions results from the ability of PrP^{Sc} to self-propagate by stimulating the misfolding of PrP^C. Spontaneous cases account for >85% of all human PrP prion disease, the most common form of which is sporadic Creutzfeldt-Jakob disease (CJD). The inherited forms account for 10–15% of all cases and are typified by Gerstmann-Sträussler-Scheinker (GSS) disease (5). The infectious form represents <1% of all cases and is epitomized by kuru that was transmitted among the Fore people of New Guinea by ritualistic cannibalism (6). Currently, there is no effective treatment for any PrP prion diseases.

CJD shares histopathological findings of aggregated misfolded protein deposits in the brain with other human neurodegenerative diseases and proteinopathies, including Alzheimer's disease (AD); Parkinson's disease (PD); tauopathies, such as frontotemporal dementia (FTD); Huntington's disease (HD); and amyotrophic lateral sclerosis (ALS) (7,8). AD, HD, PD, and tauopathies involve misprocessing of specific cellular proteins into alternate non-native isoforms that produce cellular toxicity; pathogenic proteins then propagate in a prion-like process (9–15). PrP^{Sc} forms insoluble fibrils, then aggregates, some form of which is neurotoxic (16,17). Oligomers may be more neurotoxic than aggregates although this remains controversial. Lowering levels of PrP^{Sc} in the brain by halting its formation or increasing its clearance should be therapeutically desirable.

Infectious forms of animal prions can be propagated *in vitro* in prion-infected murine neuroblastoma cell lines (ScN2a) (18). Compounds reported to be active *in vitro* in lowering PrP^{Sc} levels are known drugs approved for other indications, or small chemical sets expected to have bioactivity, based on results from cell-based assays (19–22). Drugs or experimental compounds reported to have antiprion activity include acridines (e.g., quinacrine) (23,24); tricyclic antidepressants; analogs of statins (25); pyrazolones (26); indole-3-glyoxyamides (27); and pyridyl hydrazones (28), including “Compd B.” Except for Compd B, all have failed to substantially extend survival in prion-infected animals. Larger polyanionic or polycationic compounds, or polyamidoamine dendrimers (PAMAM), have antiprion activity in cells (29), but are not practical as drugs, because of drug delivery, safety, or other issues.

Recently, we discovered a set of molecules containing the 2-aminothiazole (2-AMT) moiety using high-throughput screening (HTS) of almost 10,000 diverse chemical compounds (30) and reported medicinal chemistry efforts to identify more potent and drug-like 2-AMT analogs (31). Preliminary studies indicate that the 2-AMTs do not decrease the expression of PrP^C or denature PrP^{Sc}, suggesting that they likely exert their antiprion activity by inhibiting the formation or enhancing the clearance of PrP^{Sc} (30). Twenty-seven 2-AMT analogs were synthesized and tested *in vitro* for potency and in two rounds of PK screening. In the first round, single-dose PK studies focused on AUC, AUC/EC₅₀ ratios, and C_{max}/EC₅₀ in brain and plasma as criteria for further advancement. In the second round, 10 were evaluated in multiple-dose PK studies to determine 3-day concentrations (C_{3-day}) after dosing as part of a liquid diet. This is the least invasive way to dose mice in efficacy studies that could last up to 300 days or more. From C_{3-day} in plasma and brain, we calculated AUC and AUC/EC₅₀ ratios. IND24 and IND81 were selected for subsequent studies in prion-infected mouse models.

Success treating bacterial infection while preventing resistance is correlated with dosing regimens that achieve and maintain high multiples of AUC/MIC, time above the MIC, or both (32,33). We reasoned that if the same principles apply in the treatment of prion diseases, and *in vitro* EC₅₀ determinations have predictive value, like MIC, then IND24 and IND81 would be suitable candidates to advance, because both showed brain and plasma AUC/EC₅₀ ratios, after 3 days of dosing, greater than 100 based on total concentration, and 113 (IND24) and 48 (IND81) based on unbound brain concentration when dosed at 210 mg/kg/day.

Overall, the *in vitro* activity and high AUC/EC₅₀ ratios *in vivo* in brain and plasma for total and unbound drug predict good extension in survival for IND24 and IND81 in RML-infected mouse models of prion disease. Good extension in survival was previously reported for Compd B in an RML-

infected mouse model of prion disease (28). It would be important to compare the effects of IND24 and IND81 in the RML mouse model with Compd B serving as a positive control. Therefore, we evaluated its PK at various doses and showed that at a dose of 100 mg/kg/day, Compd B had similar AUC/EC₅₀ ratios in brain and plasma compared with IND24 and IND81 based on total and unbound concentrations. Compd B has a phenylhydrazone group, which can be activated by cytochrome P450 (CYP450) to reactive intermediates, making it potentially unsuitable as a drug for humans or animals (34). IND24 and IND81 lack a phenylhydrazone moiety and were well tolerated when dosed at 210 mg/kg/day for two weeks.

MATERIALS AND METHODS

Materials

All twenty-seven 2-AMT analogs were synthesized at small scale (up to 1 g) at the Small Molecule Discovery Center at UCSF. Lead compounds IND24 and IND81 were subsequently synthesized at 100- to 200-g scales at ChemVeda (Hyderabad, India). One hundred mg of Compd B [(E)-5-(4-(2-(pyridin-4-ylmethylene)hydrazinyl)phenyl)oxazole] along with the synthetic scheme was generously provided by Professor Katsumi Doh-ura (Tohoku University, Sendai, Japan), subsequently synthesized at UCSF, and finally scaled-up to 100 g quantities at ChemPartner (Shanghai, China). Warfarin (positive control for protein binding assay) and chlorowarfarin (internal standard for warfarin) were obtained from Toronto Research Chemicals (Ontario, Canada). Blank sodium heparinized plasma from mouse (CD-1) and human was obtained from Bioreclamation (Hicksville, NY), and Dulbecco's phosphate-buffered saline (PBS) from Invitrogen (Carlsbad, CA). The rapid equilibrium dialysis (RED) devices and reusable base plate were obtained from Thermo Scientific (Rockford, IL). Mouse, rat, and human liver microsomes were from Xenotech (Lenexa, KS).

FVB mice (bred at the Hunter's Point animal facility at UCSF or purchased from Charles River, Hollister, CA) were used for all PK studies. Dose formulations for *in vivo* PK studies contained DMSO (Thermo Fisher Scientific, Rockford, IL), propylene glycol (Sigma-Aldrich, St. Louis, MO), α -tocopheryl polyethylene glycol 1,000 succinate (TPGS; Eastman Chemical Co., Kingsport, TN), absolute ethanol (Fisher Scientific, Pittsburgh, PA), labrosol (Gattefosse, France), and polyethylene glycol 400 (PEG400; Hampton Research, Aliso Viejo, CA). Rodent liquid diet was obtained from Bio-Serv (Frenchtown, NJ). Brain tissue was homogenized using a Precellys 24 (Bertin Technologies, France) tissue homogenizer. LC/MS/MS analysis was performed using an API 4,000 triple quadrupole mass spectrometer (Applied Biosystems) with Analyst 1.4.2

software, coupled to a Shimadzu CBM-20A controller, LC20AD pumps, and SIL-5000 auto sampler (Shimadzu Scientific, Columbia, MD). Compounds were separated on either a BetaBasic C18 or a BDS Hypersil C8 column (both 3 μ m, 50 \times 2 mm; Thermo Scientific, Rockford, IL) using a gradient between 0.1% formic acid in water and 0.1% formic acid in acetonitrile (ACN). HPLC-grade ACN and water were obtained from VWR Scientific (Radnor, PA).

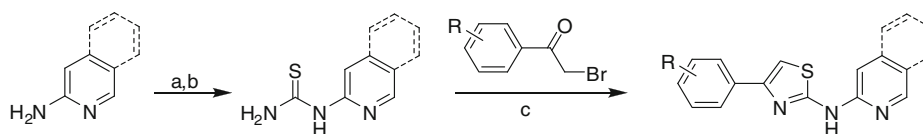
Chemistry

The general procedure for synthesis of the 2-AMTs and Compd B are depicted in Schemes 1 and 2, respectively. Details of the synthesis of the 27 2-AMTs are given in the Supplementary Material. Compd B was previously described (28) and our implementation of the synthesis, including a route to Compd B, is described in the Supplementary Material.

Cell-Based Assays

To identify and confirm hits that lower levels of PrP^{Sc}, concentration-effect (EC₅₀) curves were performed by ELISA (Lu *et al.*, *in preparation*). Mouse N2a neuroblastoma cells (ATCC) transfected with full-length mouse PrP and infected with the RML strain of mouse-adapted scrapie prions (ScN2a-cl3 cells; (35)) were seeded into black-walled, clear-bottomed, tissue culture-treated plates (Greiner) and incubated with the compounds at a final test concentration ranging from 1 nM to 10 μ M. After 5 days' incubation at 37°C in a humidified and 5% CO₂-enriched environment, lysates were generated as previously described and transferred to high-binding ELISA plates (Greiner) coated with D18 primary antibody for overnight incubation at 4°C. The next day, the plates were washed with Tris-buffered saline Tween-20 (TBST) before addition of 100 μ L of a 1:1,000 dilution of HRP-conjugated D13 antibody in 1% BSA/PBS (1-h incubation at room temperature). After incubation with the D13 antibody, the plates were washed with TBST, 100 μ L of 2,2'-azino-bis(3-ethylbenzothiazoline-6-sulphonic acid (ABTS) was added to each well for 10 min, and absorbance at 405 nm was read using a SpectraMax M5 plate reader (Molecular Devices, Sunnyvale, CA).

To evaluate cell viability (35), mouse ScN2a-cl3 cells were seeded into 96-well, black polystyrene plates (Greiner) and treated with compound as described above for the ELISA plates. After 5 days, the growth media was aspirated, the plates washed once with PBS (250 μ L/well), and the plates aspirated dry. Calcein-AM (100 μ L/well, 5 μ g/mL solution in calcium- and magnesium-free PBS) was added, and the plates were incubated at 37°C for 45 min. Fluorescent emission intensity



Scheme 1 General procedure for synthesis of antiprion 2-AMTs. Conditions: (a) BzNCS, acetone, reflux; (b) NaOH, MeOH, reflux; (c) EtOH, reflux.

was quantified using a Spectramax M5 plate reader, excitation/emission spectra of 485 nm/530 nm.

Calculated Physicochemical Parameters

Calculated physicochemical parameters for the 27 2-AMTs, including tPSA (A), xlogP, and number of hydrogen bond donors and acceptors were determined using SARvision (<http://www.chemapps.com>) to explore any relationships between physicochemical and PK parameters.

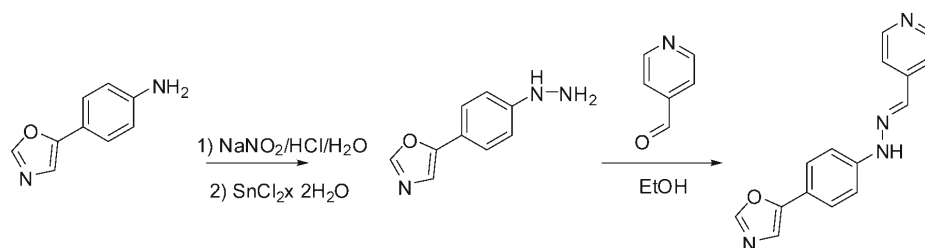
Fasted-State Simulated Intestinal Fluid Solubility

Intestinal solubility was estimated using fasted-state simulated intestinal-fluid (FaSSIF) solubility. Aliquots of the 10-mM DMSO stocks were transferred to pH 2 (HCl) buffer, pH 7.4 (phosphate) buffer with and without 0.05% polysorbate 80 (PS80), or FaSSIF to give a target concentration of 250 μ M solute and 2.5% DMSO. After equilibration at room temperature overnight, the solutions were filtered and solute concentration determined by fast gradient HPLC with UV/VIS/MS detection with reference to 1, 5, 10, 50, 100, and 250 μ M analytical standards. These analytical standards were prepared from a 500- μ M intermediate stock solution made by diluting 10 μ l of the 10-mM sample stocks into 190 μ l of 50:50 (v/v) ACN/water. Aliquots of 0.4, 2, 4, 20, 40, and 100 μ l were transferred in duplicate into a 96-well plate and the volumes were made up to 200 μ l per well with ACN/water. The plate was then heat-sealed with a foil sheet. Prior to sample filtration, filters were primed with 600 μ l of sample to resolve potential adsorption problems. Both sample replicates were collected through the primed filter. Duplicate determinations were made in all cases.

Media Solubility

To evaluate media solubility, two protocols were followed. In the first, solutions were prepared as described above.

Scheme 2 Synthesis of Compd B.



After overnight equilibration, samples were centrifuged for 30 min, without filtration, and supernatant analyzed by HPLC/UV/VIS with reference to three standards (5, 100, 250 μ M). In the second protocol, turbidimetric analysis, dilutions of the compound of interest were prepared in media with target concentrations of 5, 10, 20, 50, 100, 200, and 300 μ M. Media without solute was included for background. These solutions were evaluated using a light scattering technique and a Nepheloskan instrument. A reading that was greater than or equal to 3 times background was considered the limit of solubility.

Hepatic Microsomal Stability

Stability of nine 2-AMT compounds and Compd B were determined *in vitro* in mouse, rat, and human liver microsomes to compare rates of disappearance across species. Aliquots of DMSO solute stocks were diluted into ACN and then into assay buffer (PBS, pH 7.4, \pm 0.05% PS80). Final experimental solute concentrations were 1 μ M (0.6% ACN, 0.01% DMSO). To commercially available mouse, rat, or human hepatic microsomes (\sim 0.5 mg/mL final concentration), NADPH (1 mM) or PBS was added. The resulting mixture was incubated at 37°C, and aliquots removed at 0, 1, 10, 30, and 60 min, then quenched with ACN containing 2 μ M carbamazepine (internal standard). After centrifugation at 12,000 $\times g$ for 10 min, the supernatant was analyzed by LC/MS for remaining starting material. Duplicate incubations were run for each time-point. The percentage of solute remaining at the end of the incubation was used to determine *in vitro* half-life ($t_{1/2}$) using the calculations below (36).

$$\text{In vitro } t_{1/2} = -0.693/k$$

where (-k) is the slope of the linear regression line from the plot of log percent remaining *versus* incubation time.

Identification of Metabolites of IND24 and IND81

Metabolite identification was only performed for IND24 and IND81 because they were the only two that were selected for evaluation in RML-infected mouse models. The goal was to identify metabolites in human microsomes and determine if these would also be observed in mouse, rat, and dog. Metabolites were separated on a Kinetex 100-Å column (2.6 μm , 100 \times 2.1 mm, Phenomenex, Torrance, CA) at ambient temperature. The mobile phase consisted of 0.1% formic acid (Solvent A) and ACN (Solvent B), and was delivered at 0.200 mL/min for 50 min. The initial composition of solvent B was maintained at 1% for 5 min and then increased in a linear manner as follows: 30% at 20 min; 50% at 25 min, maintained at 50% for 3 min; and then increased to 90% at 40 min. Solvent B was maintained at 90% for up to 45 min and then decreased to 1% in the next 2 min. The column was allowed to equilibrate at 1% solvent B for 5 min prior to the next injection. The HPLC effluent going to the mass spectrometer was directed to waste through a divert valve for the initial 5 min after sample injection. Mass spectrometric analyses were performed on a ThermoFinnigan LTQ Orbitrap mass spectrometer (ThermoScientific; Waltham MA), which was interfaced to an Agilent HP-1100 HPLC system (Agilent Technologies, Palo Alto, CA) and equipped with an electrospray ionization source (ESI). The parameters for the ESI source were: capillary temperature 325°C; source voltage 3.5 kV; source current 100 μA ; capillary voltage 33.0 V. The mass spectrometer was operated in a positive-ion mode with data-dependent scanning.

The Orbitrap mass analyzer was calibrated according to the manufacturer's directions using a mixture of caffeine, Met-Arg-Phe-Ala (MRFA) peptide and Ultramark 1621. The parent compounds and their metabolites were detected by full-scan mass analysis from m/z 150–1000 at a resolving power of 60,000 [at m/z 400, full width at half maximum (FWHM); 1-s acquisition] with data-dependent MS/MS analyses triggered by the most abundant ion. This was followed by MS^3 of the most abundant product ion. The resolving power used for multiple-stage mass analysis was the same as the full-scan mass analysis. The CID was conducted with an isolation width of 3 Da, normalized collision energy of 35 for MS/MS and MS^3 , activation q of 0.25 and an activation time of 30 ms. Default automatic gain control (AGC) target ion values were used for MS, MS/MS, and MS^3 analyses. The data obtained were analyzed using Xcalibur v2.1 software (ThermoScientific; Waltham MA). Four-decimal monoisotopic masses of the parent compounds and their oxidative metabolites calculated using ChemBioDraw Ultra software version 11.0 (CambridgeSoft; Cambridge, MA) were used to interpret further the fragment ions.

Cytochrome P450 Phenotyping

Because IND24 and IND81 were the only compounds selected for *in vivo* testing in RML-infected mice, they were the only ones subjected to cytochrome P450 phenotyping. IND24 and IND81 were incubated in pooled human liver microsomes (HLMs; 0.5 mg/mL microsomal protein) in the presence or absence of selective inhibitors of P450s, specifically 10 μM furafylline with 15-min preincubation (CYP1A2), 5 μM sulfaphenazole (CYP2C9), 5 μM (+)-N-3-benzylrivanol (CYP2C19), 1 μM quinidine (CYP2D6), and 1 μM ketoconazole (CYP3A4). IND24 and IND81 concentration was 1 μM and the final organic solvent of the incubation mixture was less than 0.1%. Duplicate incubations were performed and the reaction stopped after 60 min by the addition of 0.1% formic acid in ACN containing internal standard. After vortexing and centrifugation at 12,000 $\times g$ for 10 min, the supernatant was analyzed by LC/MS/MS.

Involvement in the metabolism of a specific CYP enzyme was estimated based on the following equations:

$$\begin{aligned}\% \text{ Disappearance} &= \frac{[(\text{TC without NADPH}) - (\text{TC with NADPH})]}{(\text{TC without NADPH})} \times 100 \\ \Delta \text{ Disappearance} &= (\% \text{ Disappearance of TC in the presence of NADPH} - \% \text{ Disappearance of TC in the presence of NADPH and chemical inhibitor}),\end{aligned}$$

where TC is the test compound.

CYP450 inhibition or induction studies were not performed at this time to identify potential drug-drug interactions, because CJD is a rapidly fatal disease and dose adjustment could be made for drugs that would need to be coadministered.

Bidirectional MDCK-MDR1 Cell Permeability

Permeability studies were performed to determine which, if any, were substrates for P-glycoprotein (P-gp). MDCK-MDR1 cells were grown to confluence for 5–10 days on 1- μm filters in 24-well plates (37). Aliquots of DMSO stocks were diluted into Hank's balanced salt solution (HBSS), pH 7.4, containing 25 mM +0.05% PS80 to give 10 μM solute concentration. The solute-containing donor solutions were transferred to either the apical or basolateral chamber of the permeability diffusion apparatus. Receiver solutions consisted of HBSS (pH 7.4) containing 25 mM HEPES +0.05% PS80. Sequential samples of transported solute were taken at 20-min intervals using an automated liquid-handling platform. The concentration of transported solute during each sampling interval was determined by HPLC/

UV/MS. Permeability coefficients were calculated for each sampling interval. The average and standard deviation from the intervals are reported. Mass balance in the system was ascertained by comparing the sum of total transported solute and remaining donor solute with the starting mass of solute and is expressed as a percentage of donor solute at time zero. Significant deviations from 100% (generally less than 70%) suggest solute adsorption to the apparatus or monolayer, or chemical or metabolic instability during the course of the experiment. In the event of mass balance less than 70%, the cell monolayers were extracted with ACN and analyzed for the solute of interest. Determinations were conducted in duplicate.

Plasma Protein, Brain Tissue, and Cell-Culture Media Binding

Binding studies were only performed for IND24, IND81, and Compd B because these were the only three selected for *in vivo* evaluation in RML-infected mice, in order to ultimately evaluate *in vitro-in vivo* (IVIV) correlations based on total and unbound drug in plasma, brain tissue, and cell-culture media. Stock solutions of 0.1 mM of IND24, IND81, Compd B, and warfarin (positive control) were prepared in DMSO and diluted 100-fold in mouse and human plasma, or in mouse brain homogenate (prepared by diluting brain samples from untreated FVB mice 5-fold with water and homogenizing using a Precellys 24 tissue homogenizer), or in cell-culture media that was supplemented with 10% FBS, to yield a final concentration of 1 μ M. The final DMSO concentration in plasma was 1%. *In vitro* protein binding was determined by using a rapid equilibrium dialysis (RED) device containing a dialysis membrane with a molecular weight cut-off of ~8,000 daltons. The experiments were run in duplicate (warfarin) or triplicate (IND24, IND81, and Compd B). A 200- μ l aliquot of the spiked plasma, brain homogenate, or cell-culture media sample was placed in the sample chamber and 350 μ l of Dulbecco's PBS, pH 7.4, was placed in the buffer chamber of the insert. The unit was covered with a sealing tape and incubated at 37°C with shaking at 100 rpm for 4 h. At the end of the incubation period, 50- μ l aliquots each from the sample and buffer chambers were pipetted into separate microcentrifuge tubes. The buffer sample was diluted with 50 μ l of appropriate blank plasma/brain homogenate/cell-culture media, and an equal volume of PBS, pH 7.4, was added to the plasma/brain homogenate/cell-culture media samples. For analysis, 150 μ l of ACN containing internal standard was added to 50- μ l aliquots of the samples and centrifuged at ~12,000 $\times g$ for 10 min. The supernatants were analyzed by LC/MS/MS. Plasma protein binding and binding in cell-culture media was calculated as follows:

% Fraction unbound

$$= (\text{Buffer concentration}/\text{Plasma concentration}) \times 100$$

The fraction unbound (f_u) value in the diluted brain tissue ($f_{u_{\text{meas}}}$) was calculated as above. This was converted to the undiluted f_u value ($f_{u_{\text{brain}}}$) using the following equation (38),

$$f_{u_{\text{brain}}} = \frac{\frac{1}{D}}{\left(\left(\frac{1}{f_{u_{\text{meas}}}}\right) - 1\right) + \frac{1}{D}}$$

for which D is the dilution factor of the brain tissue.

In Vivo Studies

Single-Dose Pharmacokinetic Studies

Twenty-seven 2-AMTs and Compd B synthesized and tested for antiprion potency in dose-titration EC₅₀ studies using an ELISA-based assay were selected for first-round testing in oral PK studies at a single dose of 40 mg/kg. It was important to identify 2-AMT compounds from these studies that showed good exposure, especially in the brain, to advance to 3-day studies.

Protocols for PK studies employing mice were reviewed and approved by the UCSF Institutional Animal Care and Use Committee (IACUC). Female FVB mice, weighing approximately 25 g, were used for all *in vivo* PK studies. Mice were housed with free access to food and water, and were maintained on 12-h light/dark cycles for 1 week before dosing studies were initiated.

For the single dose of 40 mg/kg, compounds were dissolved in a formulation containing 5% propylene glycol, 35% TPGS and 60% PEG400, and administered by oral gavage. Two animals per time point were used. At specified time points after dosing (0.5, 1, 2, 4, 6, and 24 h), animals were euthanized by CO₂, and blood for plasma (by cardiac puncture) and brain samples were collected from each. The heparinized blood samples were centrifuged to obtain plasma. Brain samples were weighed, diluted 10-fold with water, and then homogenized using a Precellys 24 tissue homogenizer. The brain and plasma samples were flash-frozen on dry ice and then stored at -80°C until analysis.

IND24, IND81, and Compd B were also evaluated in single-dose PK studies at 1 mg/kg intravenous (IV) injection and 10 mg/kg oral gavage to characterize several PK parameters, including V_{ss}, CL, t_{1/2}, C_{max}, and AUC. For IV dosing through tail injection, IND81 and Compd B were dissolved in either 10% DMSO in PEG400/water (1:1) or 10% DMSO; IND24 was dissolved in 10% ethanol in PEG400/water (1:1). For the single-dose administration at 10 mg/kg, compounds were dissolved in a formulation

containing 20% propylene glycol, 5% ethanol, 5% labrosol, and 70% PEG400, and administered by oral gavage. Two animals per time point were used. At specified time points after dosing (5 min, 0.25, 0.5, 1, 2, 4, and 6 h for IV dosing, or 0.25, 0.5, 1, 2, 4, 6, and 24 h for oral dosing), animals were euthanized by CO₂. Blood and brain samples were obtained from each. The heparinized blood samples were centrifuged to obtain plasma. Brain samples were weighed, diluted five-fold with water, and then homogenized using a Precellys 24 tissue homogenizer. The brain and plasma samples were flash-frozen on dry ice and then stored at -80°C until analysis.

Multidose Pharmacokinetic Studies

Ten compounds were selected from among the 27 2-AMTs for the second round of screening in 3-day multiple-dose (MD) PK studies at PO doses of 40, 80, 130, and 210 mg/kg, chosen based on AUC and ratios of AUC/EC₅₀ and C_{max}/EC₅₀ from the single-dose experiments. We used a liquid diet to facilitate easy drug administration, as well as to serve as the daily source of all water and food. In addition, Compd B at doses of 25, 50, 100, and 150 mg/kg/day was administered for 3 days in liquid diet. This dosing approach was chosen because the mouse bioassay studies that would be used to assess drug effects on survival would be expected to run for 110 to 300 days, or more; gavage dosing for such a long period is not feasible and more stressful to mice. For the MD PK studies with the 2-AMT compounds, 4.5 g of the 2-AMT analogs was added to 15 mL of pure PEG400, vortexed, and sonicated to ensure dissolution, then stored at 4°C until needed. This highly concentrated PEG400 solution was subsequently diluted to final dosing concentrations and added to the rodent liquid diet.

Wild-type FVB mice weigh ~25 g and typically drink 20 mL of liquid diet per day, allowing an estimate of daily drug consumption. A single-dosing cohort consisted of three

mice in a shared cage and liquid diet was provided at the start of the study in sufficient volume (~200 mL) to last for the entire 3-day period. Mice typically consume their diet during the dark cycle (12 h), so while a dosing interval is 24 h, consumption of food, water, and drug occurred during a ~12 h period on each of 3 days. Three hours after the end of the final dosing period, animals were euthanized by CO₂, followed by collection of plasma (cardiac puncture) and removal of whole brain. Samples were processed and stored as described under single-dose PK studies. IND24 and IND81 were also dosed at 210 mg/kg/day for 14 days to evaluate drug tolerance; methods of administration and sample collection were as described above.

Sample Analysis

Plasma and brain homogenate samples were extracted using a protein-precipitation method and analyzed by specific LC/MS/MS methods developed for each compound dosed *in vivo*. The analytical method accuracy and precision were monitored by analyzing quality control (QC) samples that were prepared by the same methods as the plasma or brain homogenate samples. The brain and plasma concentration data were used to calculate the maximal concentration (C_{max}), area under the concentration-time curve from time 0 to the last time point (AUC_{last}), and absolute bioavailability (%F) by noncompartmental analysis with sparse sampling performed using Phoenix WinNonlin 6.1 software (Pharsight, Mountain View, CA), following single-dose studies. From the multiple-dose PK data, concentrations (C_{3-day}) in brain and plasma were determined from the samples taken 3 h after the end of the dark cycle on the third day. The AUC for plasma and brain after 3 days of oral dosing was estimated (39) as the product of C_{3-day} × τ , where τ is the dosing interval (12 h) because mice eat and drink predominantly during their dark cycle, and this would generate a more conservative estimate for AUC. We know of no other method to estimate AUC after 3 days of dosing using the liquid diet. Other approaches require an assumption of linear PK, which is not observed

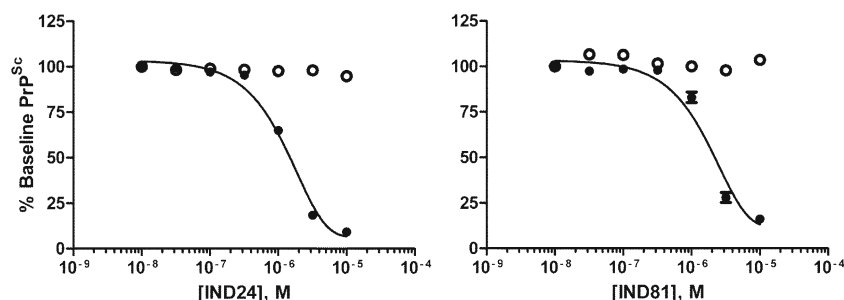


Fig. 1 Potency (EC₅₀) curves as measured by ELISA (solid circles) for IND24 (1.27 μ M and 325 nM for total and unbound compound, respectively) and IND81 (1.95 μ M and 452 nM for total and unbound compound, respectively). Cell viability by calcein (open circles) indicated that LC₅₀ values for both IND24 and IND81 were >10 μ M. Solid lines show results based on total drug. All EC₅₀ values are based on $n=3$.

Table 1 2-AMT Analogs Synthesized and Tested For Potency With Calculated Parameters

Compd	Structure	EC ₅₀ (μ M) ^a	MW	tPSA ^b	xlogP	HBA/ HBD ^c	Compd	Structure	EC ₅₀ (μ M) ^a	MW	tPSA ^b	xlogP	HBA/ HBD ^c
IND2		1.66	297.4	47.0	4.41	4/1	IND48		>10.0	283.4	58.0	4.07	4/2
IND7		1.00	268.3	50.7	3.05	4/1	IND49		>10.0	283.4	58.0	4.07	4/2
IND22		1.46	307.4	51.3	5.17	4/1	IND52		4.95	268.3	50.7	3.13	4/1
IND24		1.27	343.4	37.8	6.27	3/1	IND57		>10	325.4	56.3	3.95	5/1
IND26		>10.0	351.4	47.0	5.81	4/1	IND64		0.85	368.8	64.1	4.91	5/1
IND29		1.57	268.3	50.7	3.13	4/1	IND74		3.13	327.4	56.3	4.37	5/1
IND33		0.94	334.4	64.1	4.29	5/1	IND76		1.23	350.5	50.7	4.83	4/1
IND36		>32.0	348.4	64.1	4.57	5/1	IND78		>32.0	351.4	47.0	5.81	4/1
IND38		2.29	292.4	61.6	4.16	4/1	IND81		1.95	350.5	50.7	4.83	4/1
IND42		1.00	327.4	56.3	4.37	5/1	IND82		15.6	314.4	69.2	2.78	6/1
IND43		2.53	381.4	56.3	5.08	5/1	IND85		0.31	304.4	50.7	4.14	4/1
IND44		0.99	343.4	65.5	4.05	6/1	IND86		0.34	333.4	47.0	5.41	4/1
IND46		0.11	363.4	56.3	5.38	5/1	IND91		0.92	343.4	51.3	6.25	4/1
IND47		0.43	363.4	56.3	5.51	5/1	Compd B		0.25	264.3	63.6	2.62	5/1

^a EC₅₀ values usually based on n = 3 or more^b tPSA = total polar surface area relating to N and O atoms (TPSA_NO) as calculated in Vortex v2011, Dotmatics Limited^c HBA = H-bond acceptor; HBD = H-bond donor

based on plasma or brain concentrations at the dose of 210 mg/kg/day when compared with the 3-day data at

40 mg/kg or based on single-dose findings after doses of 10 or 40 mg/kg. The ratios of AUC/EC₅₀ were determined from

Table II Solubility and Permeability in MDCK-MDR1 Cells of 9 Selected 2-AMT Compounds

Compound	Solubility (μM)				Permeability in MDCK-MDR1 cells		
	pH 2.0	pH 7.4	FaSSIF ^a	Media ^b	P_{app} (A-B) $\times 10^{-6} \text{ cm/s}$	P_{app} (B-A) $\times 10^{-6} \text{ cm/s}$	Efflux ratio
IND22	12	<1	59	20	9.5	8.4	0.9
IND24	1	<1	118	>250	5.6	7.3	1.3
IND33	1	<1	70	225	6.8	8.3	1.2
IND44	1	<1	<1	3	20.1	24.4	1.2
IND46	<1	<1	5	174	13.2	10.5	0.8
IND47	<1	<1	5	52	9.2	8.9	1
IND52	215	1	2	76	36.2	48.7	1.3
IND81	78	<1	3	207	16	20.9	1.3
IND85	196	<1	3	116	3.03	4.44	1.5

^aFasted-state simulated intestinal fluid^bMedia used in the cell-based assays

total or unbound drug concentrations in plasma, brain, and cell-culture media. For the unbound ratios, we used unbound concentrations for both AUC and EC_{50} , after appropriate corrections for binding. The $\text{C}_{3\text{-day}}$ measured and the AUC values estimated are lower than those observed at the end of the dosing interval because the brain and plasma samples were collected 3 h after the end of dosing (the light cycle began at 6:00 AM; brain and plasma samples were collected at 9:00 AM.)

LC/MS Assays

For LC/MS quantification for all 2-AMTs, samples and their respective internal standards were injected into either a BetaBasic C18 or BDS Hypersil C8 column. The solvent system used for separation was composed of water and ACN containing 1% formic acid. For quantification of IND24 and IND81, samples (along with a proprietary internal standard) were injected onto a BetaBasic C18 column maintained at room temperature.

Table III Metabolic Stability of 9 Selected 2-AMT Compounds and Compd B

Compound	$t_{1/2}$ in min (% remaining after a 60-min incubation)		
	Mouse	Rat	Human
IND22	49 (40)	>60 (64)	>60 (99)
IND24	>60 (89)	>60 (90)	>60 (105)
IND33	>60 (111)	>60 (73)	54 (42)
IND44	29 (24)	45 (39)	58 (48)
IND46	>60 (58)	>60 (61)	>60 (83)
IND47	>60 (56)	>60 (50)	>60 (113)
IND52	6 (0)	16 (8)	36 (30)
IND81	19 (10)	58 (48)	52 (48)
IND85	15 (6)	18 (32)	53 (66)
Compd B	30 (29)	>60 (77)	>60 (68)

The amount of ACN in the gradient was increased from 75% ACN to 95% ACN over 2.5 min, held for 0.5 min, and then re-equilibrated to 75% ACN over 1.4 min. Data acquisition used MRM in the positive-ion mode, and the transitions monitored were m/z 344 \rightarrow 226 for IND24; m/z 351 \rightarrow 233 for IND81; and m/z 363 \rightarrow 245 for internal standard.

For quantification of Compd B, samples (along with a proprietary internal standard) were injected onto a BDS Hypersil C8 column maintained at room temperature. The amount of ACN in the gradient was increased from 25% ACN to 95% ACN over 2.0 min, held for 1.0 min, and then re-equilibrated to 25% ACN over 1.4 min. Data acquisition used MRM in the positive-ion mode, and the transitions monitored were m/z 265 \rightarrow 160 for Compd B and m/z 321 \rightarrow 253 for internal standard.

Table IV Fraction Unbound of IND24, IND81, and Compd B in Mouse Brain Homogenate, Mouse and Human Plasma, and Cell-Culture Media at 1 μM . Mean Percentage \pm SD Based on $n=3$, Except For Warfarin Where $n=2$

Compound	Sample	Unbound (%)
IND24	Mouse Plasma	6.63 \pm 1.55
	Mouse Brain Homogenate	8.20 \pm 0.35
	Human Plasma	4.91 \pm 1.03
	Cell-culture Media	25.7 \pm 4.93
IND81	Mouse Plasma	6.48 \pm 1.10
	Mouse Brain Homogenate	9.43 \pm 1.49
	Human Plasma	5.78 \pm 3.21
	Cell-culture Media	23.2 \pm 2.68
Compd B	Mouse Plasma	9.06 \pm 2.31
	Mouse Brain Homogenate	11.4 \pm 2.89
	Human Plasma	2.10 \pm 1.11
	Cell-culture Media	36.5 \pm 3.30
Warfarin	Mouse Plasma	10.8 \pm 0.0044
	Human Plasma	0.68 \pm 0.0023

RESULTS

Antiprion Potency and Calculated Physicochemical Parameters

Potency was defined as the EC_{50} value, calculated as the total or unbound drug concentration at which there was a 50% reduction in PrP^{Sc} levels. We chose to define potency in terms of EC_{50} and not IC_{50} values since IC_{50} estimates are traditionally used where a specific target is to be inhibited. When we measured changes in PrP^{Sc} levels, we did not know the specific target. We defined the concentration producing a 50%

reduction in PrP^{Sc} as the EC_{50} value, in a target-agnostic paradigm for which such values were determined irrespective of effects on cell viability ($EC_{50} > 10 \mu M$). Figure 1 depicts EC_{50} curves and extrapolated values for IND24 ($1.27 \mu M$) and IND81 ($1.95 \mu M$) based on total compound concentration. Corresponding values for unbound concentrations, after correcting for protein binding, are 325 and 452 nM, respectively. Concentration-effect relationships (EC_{50}) were obtained using eight concentrations per curve ranging from 10 nM to 32 μM , increasing by half-log increments. The EC_{50} values and physicochemical parameters for the twenty-seven 2-AMT compounds and Compd B are shown

Fig. 2 Metabolic profile (UV chromatogram at 268 nm) of IND24 in human, mouse, rat, and dog liver microsomal incubations (a). The parent drug is not shown in the chromatogram. Metabolites M2, M3, and M4 had the same mass spectrum as depicted in Table VI. Extracted ion chromatogram and mass spectrum of unchanged IND24 following liver microsomal incubations (b).

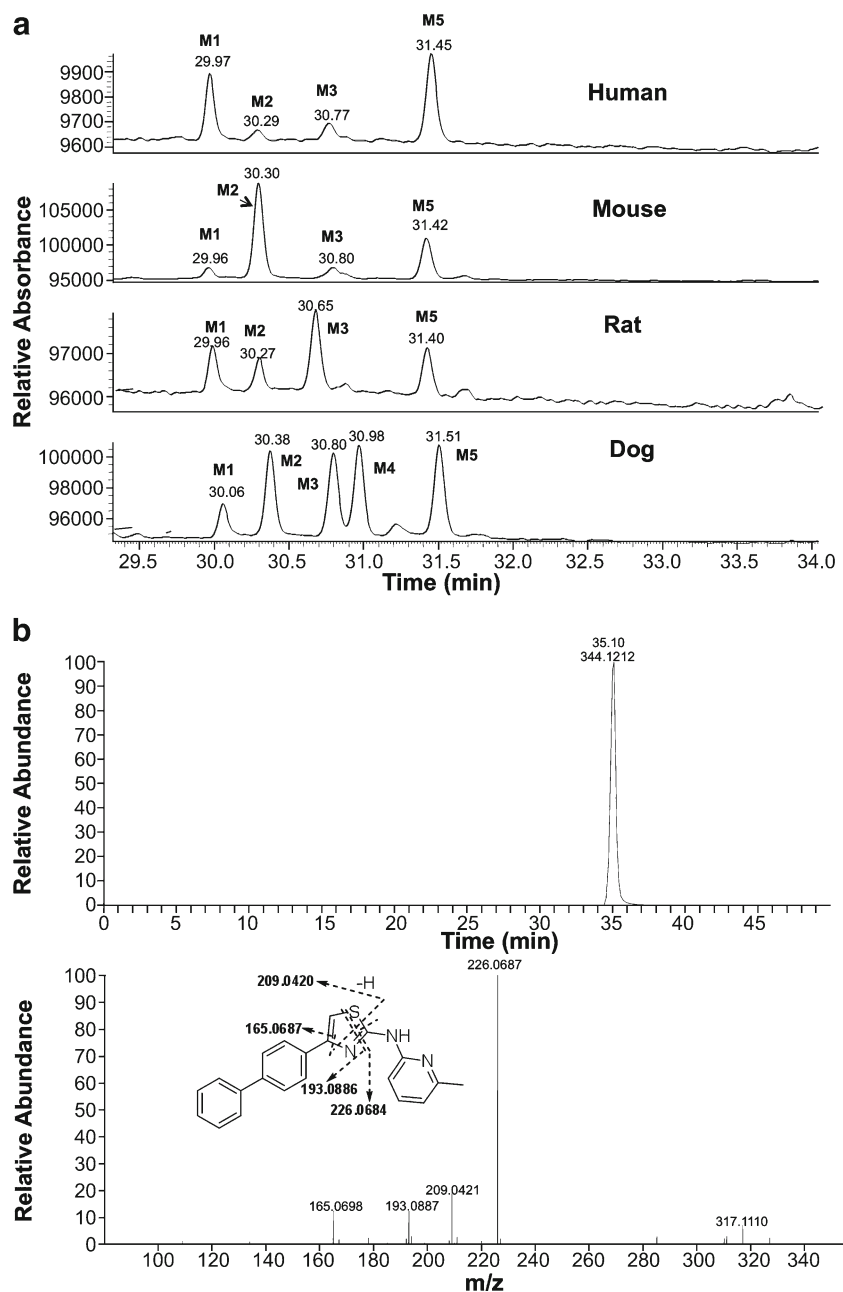


(Table I). Calculated parameters included total polar surface area (tPSA), xlogP, and number of hydrogen bond donors and acceptors. The calculated values, such as xlogP and PSA, were generally within the range of acceptable values for CNS drugs.

Solubility

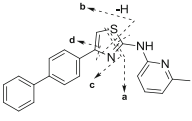
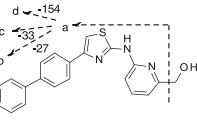
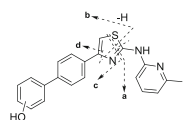
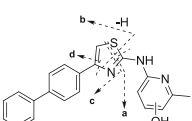
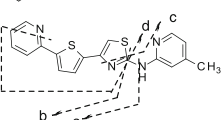
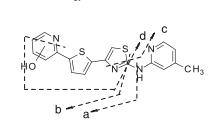
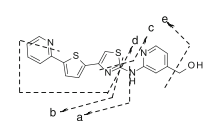
Determinations of solubility at pH 2.0 and pH 7.4 in FaSSIF, and in cell-culture media supplemented with 10% FBS were performed for nine selected 2-AMT compounds (Table II). All nine of the 2-AMTs exhibited poor solubility at pH 7.4, but good solubility in the cell-culture media containing proteins. IND22 had high solubility at both pH 2.0 and in FaSSIF. Among the others tested, IND44, IND46, and IND47 had poor solubility at both pH 2.0 and in FaSSIF. Some, like IND81 and IND85, had good solubility at pH

2.0 but poor solubility in FaSSIF, whereas others, like IND24 and IND33, had high solubility in FaSSIF but low solubility at pH 2.0. The pH-dependent solubility is most likely related to the pK_a values for each compound and the improved solubility in cell-culture media is most likely related to enhanced solubility in the presence of proteins that bind them.

Bidirectional MDCK-MDR1 Cell Permeability

Next, we evaluated whether any of the nine 2-AMTs are substrates for P-gp, which is an efflux transporter in the blood–brain barrier and intestinal wall. Permeability of the nine select 2-AMTs was evaluated in MDCK-MDR1 cells (Table II). The apparent permeability (P_{app}) values ranged from 3 to 49 ($\times 10^{-6}$ cm/sec). Efflux ratios of the compounds ranged from 0.8 to 1.5, indicating that none are substrates for P-gp.

Table V Observed (Obs.) and Calculated (Calc.) Molecular Ions And Mass Spectral Fragment Ions of IND24 and its Metabolites (top panel), and IND81 and its Metabolites (bottom panel) Following Incubation With Human, Mouse, Rat, and Dog Liver Microsomes

Metabolite	Structure		Molecular Ions	Fragment Ions					
				MH ⁺	a	b	c	d	e
Parent IND24		Obs.	344.1212	226.0687	209.0421	193.0887	165.0698		
		Calc.	344.1216	226.0684	209.0420	193.0886	165.0687		
M1		Obs.	360.1162	342.1060	315.0951	309.1262	161.0167		
		Calc.	360.1165	342.1059	315.0950	309.1260	161.0167		
M2/M3/M4		Obs.	360.1158	242.0634	225.0369	209.0835	181.0647		
		Calc.	360.1165	242.0634	225.0363	209.0835	181.0647		
M5		Obs.	360.1160	226.0686	209.0421	193.0886	165.0698		
		Calc.	360.1165	226.0684	209.0420	193.0886	165.0687		
Parent IND81		Obs.	351.0729	243.0048	233.0205	218.0096	206.0095		
		Calc.	351.0732	243.0039	233.0202	218.0092	206.0092		
M1/M3		Obs.	367.0680	258.9997	249.0154	234.0045	222.0045		
		Calc.	367.0681	258.9988	249.0150	234.0042	222.0041		
M2		Obs.	367.0679	243.0048	233.0204	218.0095	206.0094	349.0576	
		Calc.	351.0732	243.0039	233.0202	218.0092	206.0092	349.0579	

Stability in Liver Microsomes

The nine 2-AMTs and Compd B were evaluated for hepatic microsomal stability using mouse, rat, and human liver microsomes. As shown in Table III, IND24 appeared to be relatively stable in all 3 species tested, with a $t_{1/2}$ of >60 min. A few of the 2-AMTs, like IND33, IND46, and IND47, were also relatively stable in the 3 species tested, whereas others like IND85 and IND52 appeared to be rapidly metabolized. Compd B appeared relatively stable in human and rat, but was rapidly metabolized in mouse liver microsomes. There was a good correlation between the hepatic microsomal intrinsic clearance values and *in vivo* clearance values for IND24 and IND81, for which these data were available (data not shown). This would seem to indicate that *in vitro* hepatic microsomal assays might help in predicting *in vivo* clearances for other compounds with the 2-AMT scaffold.

Plasma Protein, Brain Tissue, and Cell Culture Binding

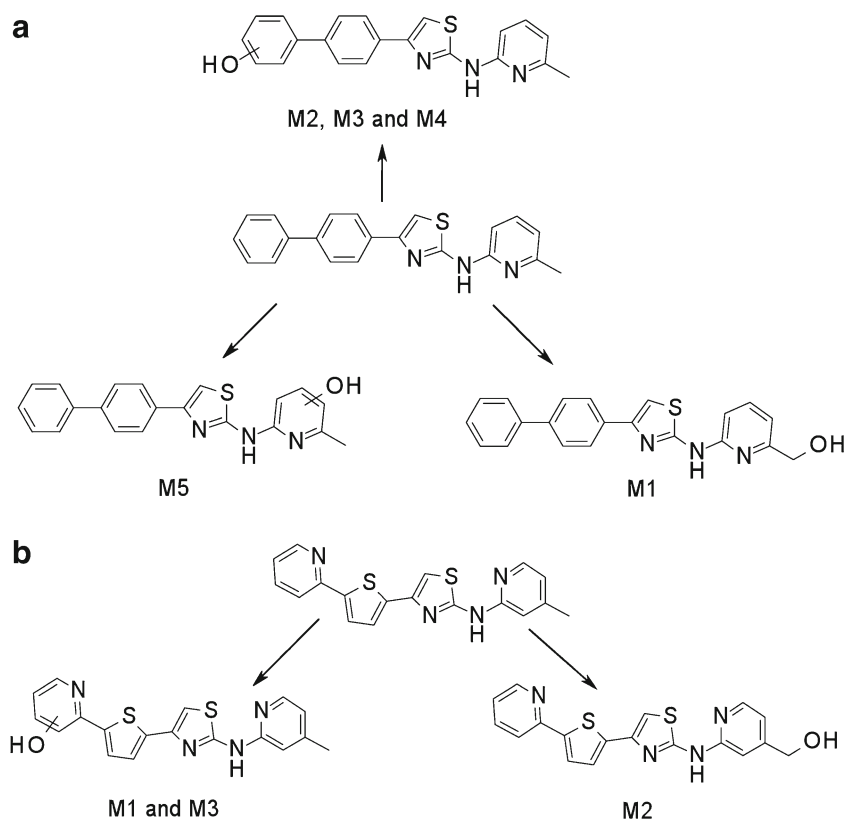
Because we were only advancing IND24 and IND81 to mouse models of prion disease, along with Compd B as a positive control, we evaluated each for binding in plasma, brain homogenates, and in the cell-culture media used for determining EC_{50} in the ELISA assays, which was supplemented

with 10% FBS (Table IV). This was done at a concentration of 1 μ M, approximating the EC_{50} concentration, using rapid equilibrium dialysis (RED). The fraction unbound for IND24, IND81, and Compd B was 6.6, 6.5, and 9% in mouse plasma, and 4.9, 5.8, and 2.1% in human plasma, respectively. Fraction-unbound values for warfarin, a control, were in good agreement with the published literature. Fraction unbound in mouse brain tissue was 9% for IND81, 8% for IND24, and 11% for Compd B. In the cell-culture media, the unbound fraction for IND24, IND81, and Compd B was 26%, 23%, and 37%, respectively. It is important to use the corresponding values when calculating AUC values in plasma and brain tissue and for EC_{50} values to determine the ratios of AUC/ EC_{50} based on unbound concentrations.

Identification of Metabolites of IND24 and IND81

To identify the metabolic profile for IND24 and IND81, we incubated these compounds (10 μ M) with human, mouse, rat, and dog liver microsomes, then scanned samples by LC/MS/MS. The structures of the metabolites were characterized using an Orbitrap mass spectrometer and by comparison with the mass spectrum of the parent compound. For IND24, metabolites M1–M3 and M5 were observed in all of the microsomal assays while M4 was only observed in the dog liver microsomal incubation (Fig. 2a). Unchanged compound IND24 eluted at 35.1 min and gave a protonated molecular

Fig. 3 Metabolic schemes of IND24 (a) and IND81 (b) following incubation with human, mouse, rat, and dog liver microsomes. For IND24, metabolite M4 was only observed following incubation with dog liver microsomes.

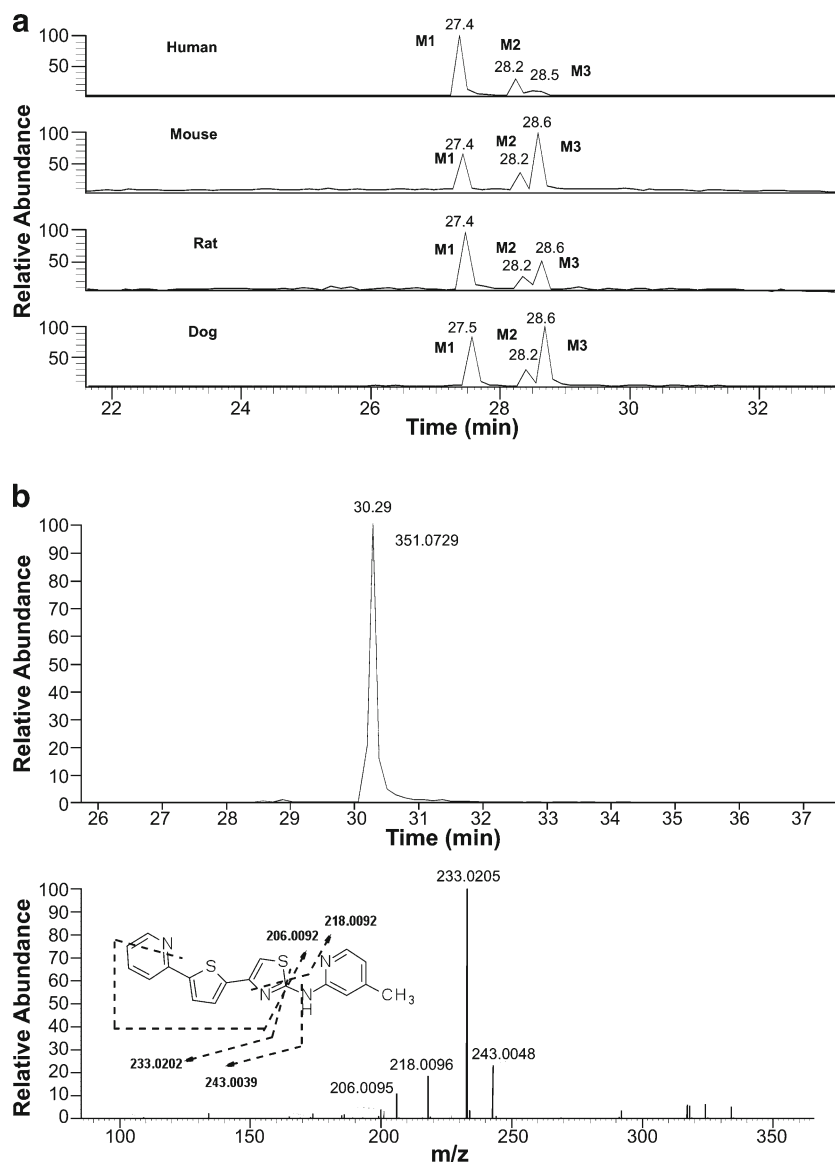


ion (MH^+) at m/z 344.1212 (Fig. 2b). The mass spectrum of MH^+ ion at m/z 344.1212 gave fragment ions at m/z 226.0687, 209.0421, 193.0887, and 165.0698 (Fig. 2b, Table V). These fragment ions were most likely formed via cleavage of the thiazole moiety because their masses were similar to the calculated masses (Table V and Fig. 2b). The peaks at 30 (M1), 30.3 (M2), 30.8 (M3), 31 (M4), and 31.5 (M5) min gave a MH^+ ion at m/z 360, an addition of 16 amu to 344, suggesting hydroxylation of the parent. The mass spectrum of M1 at m/z 360.1162 showed a major fragment ion at m/z 342.1060 in the MS/MS mass spectrum (Table V). Further fragmentation of the ion m/z 342.1060 in a data-dependent manner (MS^3) resulted in major ions at m/z 315.0951, 309.1262, and 161.0167. The ion at m/z 342.1060 resulted from loss of a water molecule from m/z 360.1162; a loss of a water molecule suggests that either the sulfur atom of the thiazole moiety or the methyl group

on the pyridine ring was hydroxylated. The exact masses of the fragment ions at m/z 315, 309, and 161 were also in good agreement with the calculated exact masses (Table V). It is well known that the S-oxides formed via oxidation of thiophene rings are generally unstable (40). The same probably applies to the thiazolyl S-oxides. Hence, the site of hydroxylation in metabolite M1 is proposed to be the methyl group on the pyridine ring (Fig. 3).

For M2, M3, and M4 of IND24, the mass spectrum of MH^+ at m/z 360.1158 resulted in fragment ions at m/z 242.0634 and 225.0369, and m/z 209.0835 and 181.0647 in the MS/MS and MS^3 spectra, respectively. An addition of 16 amu indicated an insertion of oxygen into the molecule, but the lack of an ion resulting from loss of a water molecule in the mass spectra suggested that either the biphenyl ring or the pyridine ring of the 2-methylaminopyridine moiety was

Fig. 4 Extracted ion chromatograms of oxidative metabolites of IND81 at m/z 367 following its incubation with human, mouse, rat, and dog liver microsomes (a). The UV chromatogram of the metabolic profile could not be obtained due to low intensity of the metabolites in the incubation mixture. Extracted ion chromatogram and mass spectrum of IND81 following incubation with liver microsomes (b).



modified. Modification of the methylpyridine group was ruled out by the ions at m/z 242, 225, 209, and 181, which showed an addition of 16 amu to the masses of the fragment ions observed in the mass spectrum of the parent compound. The observed exact masses of the ions were also in good agreement with the calculated exact masses for the projected fragment ions (Table V). This observation suggests modification of the biphenyl ring in all metabolites (Fig. 3). Although the spectra of the metabolites indicated modification of the biphenyl ring, the exact position of hydroxylation on this moiety could not be determined. Because the mass spectra of M2, M3, and M4 were similar, the metabolites are assumed to be regioisomers. The mass spectrum of M5 at m/z 360.1160 gave fragment ions at m/z 226.0686, 209.0421, 193.0886, and 165.0698 that were consistent with those observed in the mass spectrum of the parent compound. Similarity between the fragment ions from the spectra of M5 and the parent IND24, and the lack of loss of a water molecule for M5, suggest hydroxylation of the pyridine ring of the methylpyridine moiety (Fig. 3).

For IND81, metabolites M1–M3 were observed in microsomes of all species evaluated (Fig. 4a). Unchanged compound IND81 eluted at 30.3 min and gave a MH^+ ion at m/z 351.0729 (Fig. 4b). The mass spectrum of MH^+ ion at m/z 351.0729 gave fragment ions at m/z 243.0048, 233.0205, 218.0096, and 206.0095 (Fig. 4b, Table V). The ion at m/z 243.0048 was a result of the cleavage of the bond between the amino group of the aminomethylpyridine ring and the thiazole ring (Fig. 3b, fragment ion a, Table V). Other fragment ions were most likely generated via cleavage of the thiazole moiety, as their observed masses were similar to the calculated masses of these fragment ions. The peaks at 27.4 (M1), 28.2 (M2), and 28.5 (M3) min gave

a molecular ion at m/z 367, an addition of 16 amu to m/z 351, suggesting hydroxylation of the parent IND81. The mass spectra of M1 and M3 at m/z 367.0680 were similar and showed fragment ions at m/z 258.9997, 249.0154, 234.0045, and 222.0045 (Table V). All fragment ions indicated an addition of 16 amu to the masses of the fragment ions observed in the mass spectrum of the parent compound. The observed exact masses of the ions were also in good agreement with the calculated exact masses for the projected fragment ions (Table V). This similarity suggests that the thienylpyridine ring of IND81 is the site of modification (Fig. 3). However, the exact site of oxidation could not be elucidated from this spectral information. Because the mass spectra of M1 and M3 were similar, the metabolites are assumed to be regioisomers. The mass spectrum of M2 at m/z 367.0679 gave fragment ions at m/z 243.0048, 233.0202, 218.0092, 206.0092, and 349.0579 (Table V). While the first four ions were consistent with those observed in the mass spectrum of the parent compound, the ion at m/z 349 indicated a loss of water from the molecule. The observation of the loss of water in the mass spectrum and the consistency of fragmentation of M2 with that of the parent suggest that the methyl group on the pyridine ring is the site of oxidation (Fig. 3b).

Human P450 Isoforms Involved in Metabolism of IND24 and IND81

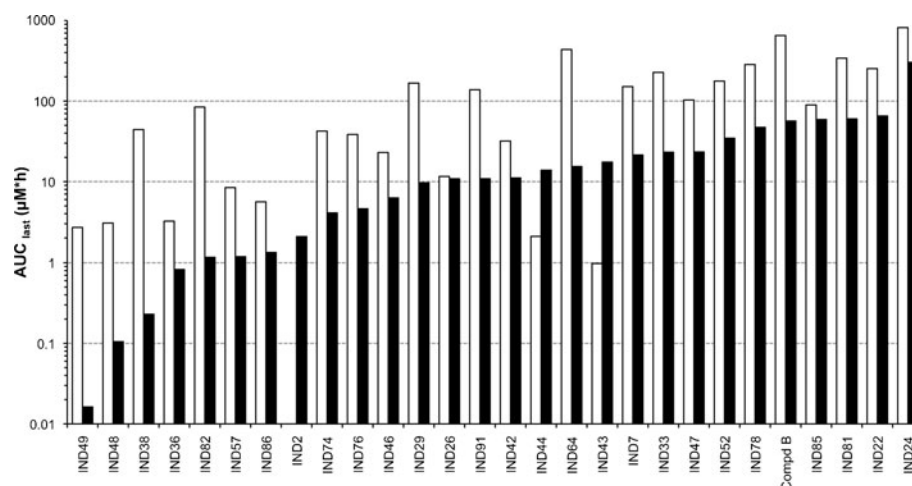
To determine which P450 isoforms are involved in the metabolism of IND24 and IND81, different P450 chemical inhibitors were coincubated with the 2-AMTs in human liver microsomes (HLMs). As has been observed previously, there

Table VI CYP Phenotyping of IND24 and IND81 at 1 μM in Human Liver Microsomes

Enzyme	Treatment	IND24				CYP?	IND81			
		Measured Conc. (μ M)	Disappearance		Measured Conc. (μ M)		Disappearance			
			%	% Δ^a			%	% Δ^a		
Irreversible incubation condition										
Negative Control	No NADPH/No Inhibitor	0.622				0.899	0			
Maximum Metabolism	NADPH/No Inhibitor	0.733	0 (–18)	0		0.143	84	0		
CYP1A2	NADPH + Furafylline	0.766	0 (–23)	0	Unlikely	0.534	41	43		Unlikely
Reversible incubation condition										
Negative Control	No NADPH/No Inhibitor	0.654	0			0.664	0			
Maximum Metabolism	NADPH/No Inhibitor	0.655	0	0		0.226	66	0		
CYP2C9	NADPH + Sulphaphenazol	0.566	14	0 (–14)	Unlikely	0.238	64	1.8		Unlikely
CYP2C19	NADPH + N-3-B	0.537	18	0 (–18)	Unlikely	0.283	57	8.5		Possible
CYP2D6	NADPH + Quinidine	0.555	15	0 (–15)	Unlikely	0.300	55	11		Likely
CYP3A4	NADPH + Ketoconazole	0.557	15	0 (–15)	Unlikely	0.324	51	15		Likely

^a The involvement of the CYP considered unlikely for values <5; possible for values 5–10; and likely for values >10

Fig. 5 Brain (black) and plasma (white) area under the curve (AUC_{last} [$\mu M \cdot h$]) for 2-AMTs and Compd B after a single 40 mg/kg oral dose.



was very little metabolism of IND24 (1 μM) in the HLM incubations, either in the presence or absence of any CYP inhibitors (Table VI). Therefore, the role of any specific P450 isozymes in the metabolism of IND24 could not be determined. In contrast, IND81 was metabolized in HLM with relatively high turnover (Table VI). Based on the change in percentage disappearance, the P450 isozymes most likely to be involved in the metabolism of IND81 are CYP2D6 and CYP3A4; CYP2C19 might be involved to a smaller extent, and CYP1A2 and CYP2C9 are unlikely to be involved.

Single-Dose Pharmacokinetics

Brain and plasma concentrations (AUC_{last} and C_{max} values) spanned four orders of magnitude across the 27 2-AMT analogs and Compd B dosed at 40 mg/kg (Fig. 5). IND48 and IND49 had the lowest AUC_{last} values; this observation is not surprising because they were the only two compounds examined that had more than one hydrogen bond donor. Both IND24 and IND81 showed very good brain and plasma exposure, with brain/plasma AUC_{last} ratios of 2.6

and 5.5, respectively, compared to a ratio of 0.5 for Compd B (Table VII). Comparison of the calculated PSA values (Table I) to the observed AUC_{last} values (Fig. 5) showed only a modest correlation. The majority of the 2-AMT analogs had maximal brain and plasma concentrations (C_{max} values) and AUC values that far exceeded their *in vitro* EC_{50} values (Fig. 6; see Table I for EC_{50} values). For many analogs at the 40 mg/kg dose, especially IND24 and IND81, the AUC_{last}/EC_{50} ratio was greater than 50 in brain and greater than 100 in plasma (Fig. 6).

Following 1 mg/kg IV dose, the half-life of IND24 was 2 h, which was 2 \times and 10 \times longer than that of IND81 and Compd B, respectively (Table VII). IND24 also had higher oral bioavailability (40%) compared to IND81 (27%) and Compd B (25%).

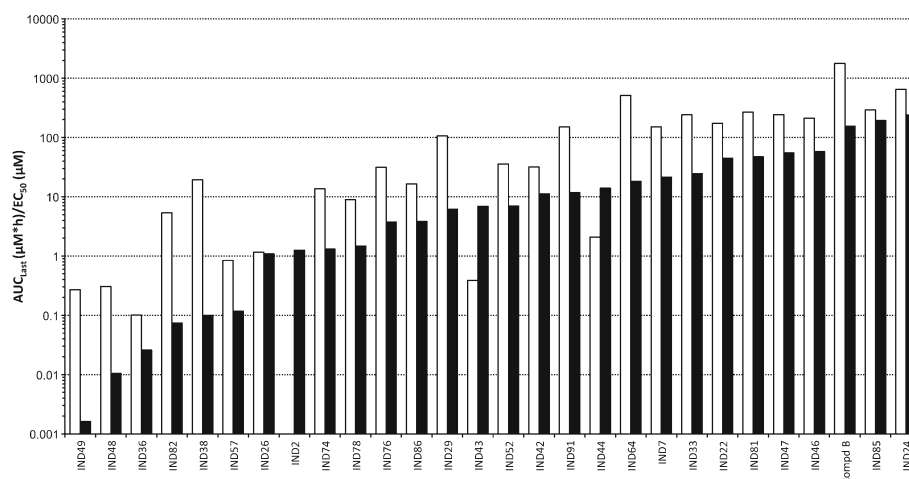
Multidose Pharmacokinetics

The 2-AMT analogs were administered at 40, 80, 130, and 210 mg/kg/day to FVB mice for 3 days in a liquid diet, then brain and plasma were collected 3 h after the end of the last

Table VII Single-Dose Plasma and Brain Pharmacokinetics of IND24, IND81, and Compd B in Female FVB Mice. Intravenous (IV) Dose was 1 mg/kg; Dose by Oral Gavage (PO) was 10 mg/kg. Mean \pm SD Shown for C_{max} and AUC Value ($n=2$)

Compd	Route/Matrix	V_{ss} (L/kg)	CL (L/h/kg)	$t_{1/2}$ (h)	C_{max} (μM)	t_{max} (h)	AUC_{last} ($\mu M \cdot h$)	%F	Brain/Plasma AUC_{last} Ratio
IND24	IV/Plasma	2.46	0.92	2.16	2.49 ± 2.65	0.083	2.78 ± 1.09	—	—
	PO/Plasma	—	—	4.65	1.66 ± 0.11	2	11.2 ± 1.31	40.3	—
	PO/Brain	—	—	nd	2.45 ± 0.74	4	29.1 ± 1.24	—	2.60
IND81	IV/Plasma	12.6	9.05	1.18	0.52 ± 0.28	0.083	0.30 ± 0.04	—	—
	PO/Plasma	—	—	0.98	0.43 ± 0.03	0.5	0.82 ± 0.39	27.3	—
	PO/Brain	—	—	1.46	1.62 ± 0.54	0.5	4.54 ± 2.28	—	5.53
Compd B	IV/Plasma	1.53	4.56	0.22	1.76 ± 0.14	0.083	0.83 ± 0.12	—	—
	PO/Plasma	—	—	1.01	0.83 ± 0.38	0.5	2.06 ± 0.06	24.8	—
	PO/Brain	—	—	nd	0.46 ± 0.16	2	1.06 ± 0.10	—	0.51

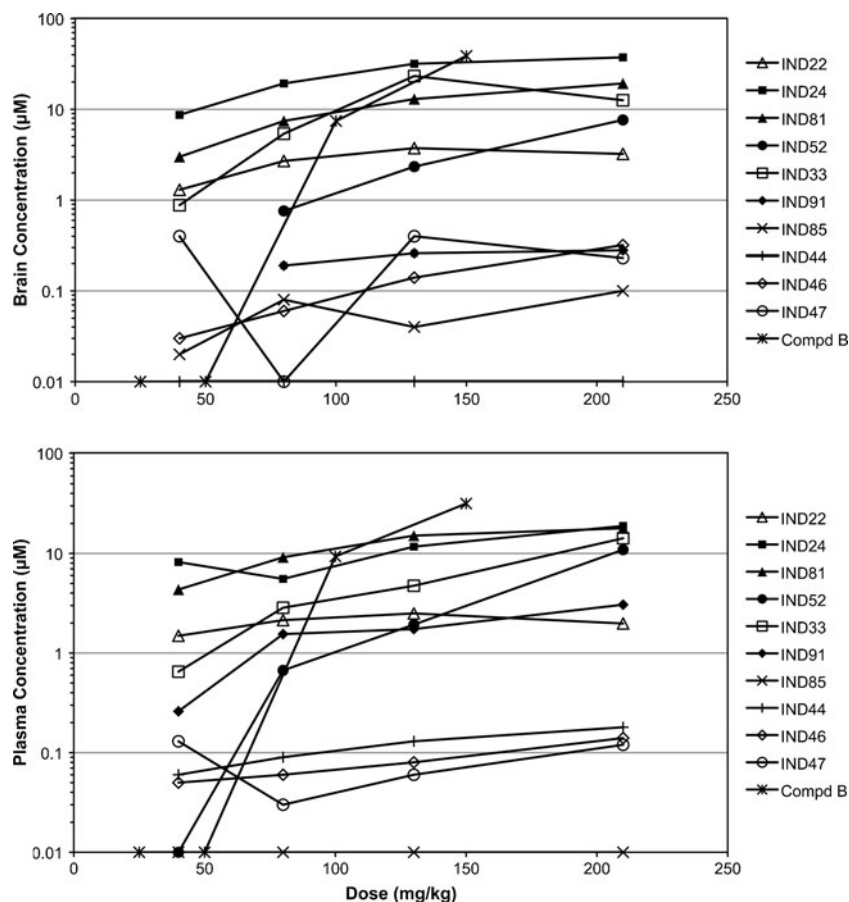
Fig. 6 The ratios of AUC [$AUC_{last} (\mu M \cdot h)$] to EC_{50} in brain (black) and plasma (white) for 2-AMTs and Compd B after a single 40 mg/kg oral dose.



dark cycle. IND24, IND81, and IND33 achieved the highest concentrations in both brain and plasma for doses greater than 40 mg/kg (Fig. 7). For IND24, both brain and plasma concentrations appeared to approach a plateau at 130 mg/kg, although it was highest at 210 mg/kg. IND81 showed higher but nonlinear increases in brain and plasma with increasing doses. IND33 showed a dose-dependent increase in plasma, but peaked at $\sim 30 \mu M$ with the 130 mg/kg dose in brain. IND52 had no measurable brain

concentrations at a dose of 40 mg/kg, while exposure was comparable at all other doses. IND22 showed comparable brain and plasma concentrations at all doses. The brain and plasma concentrations of 5 analogs (IND85, IND44, IND46, IND47, IND91) were too low ($\leq 1 \mu M$) to be of therapeutic value. A toleration study, in which mice were dosed with IND24 and IND81 at 210 mg/kg/day for 14 days, indicated that these compounds were well tolerated (data not shown).

Fig. 7 $C_{3\text{-day}}$ concentrations of ten 2-AMT compounds and Compd B in brain (top) and plasma (bottom) following 3-day dosing in liquid diet. Doses were 40, 80, 130, and 210 mg/kg/day for the 2-AMT compounds, and 25, 50, 100, and 150 mg/kg/day for Compd B. Mean values ($n=3$) are plotted; mean \pm SD values are shown in the Supplementary Material Table. In several instances, concentrations at low doses were below the lower limit of quantification by LC/MS/MS; these brain concentrations appear as missing values.



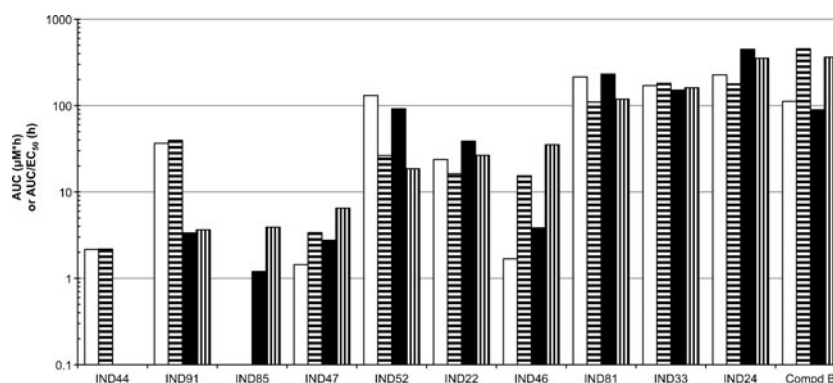


Fig. 8 AUC values for brain (black) and plasma (white) and AUC/EC₅₀ ratios for brain (vertical stripes) and plasma (horizontal stripes) based on brain and plasma concentrations for ten AMT analogs and Compd B. Values are based on a dose of 210 and 100 mg/kg/day given for 3 days for the AMT analogs and Compd B, respectively. AUC values calculated from $C_{3\text{-day}} \times \tau$, as described in the *Methods*.

Additionally, the PK of Compd B was evaluated to determine the suitable dose for use as a positive control in RML-infected mice. Doses of 25, 50, 100, and 150 mg/kg were administered to FVB mice for 3 days in a liquid rodent diet, and then brain and plasma concentrations measured (Fig. 7). Brain and plasma concentrations were below the level of quantification at the 25 and 50 mg/kg/day doses. All animals had measurable levels at 100 mg/kg/day and none showed lethal toxicity at doses of 25, 50, and 100 mg/kg/day. In contrast, two of four mice dosed at 150 mg/kg/day for 8 days died, leaving only two animals to assess drug exposure (Supplementary Material Table).

The AUC and AUC/EC₅₀ ratios for plasma and brain after 3-day dosing of IND24 and IND81 at 210 mg/kg/day or 100 mg/kg/day of Compd B were calculated from the $C_{3\text{-day}}$ values multiplied by the dosing interval (τ) (Fig. 8). The AUC/EC₅₀ ratios for IND24, IND81, and Compd B were all greater than 100 based on total concentrations in plasma and brain. After correction for binding of the compounds to proteins in

brain homogenate, the AUC/EC₅₀ ratios in brain (Fig. 9) were 113, 144, and 48 for IND24, Compd B, and IND81, respectively.

DISCUSSION

No approved drug exists for human use that slows CJD, or any of the other PrP prion disorders. We previously reported the identification of diverse chemical leads that have good potency in reducing PrP^{Sc} in prion-infected mouse neuronal cells, including a 2-AMT series (30). Subsequently, we described structure-activity relationships in the 2-AMT series and the identification of more potent and drug-like analogs (31). To date, 235 analogs in the 2-AMT series have been synthesized and evaluated for antiprion potency (EC₅₀).

The goal of the present work was to select two to three compounds for testing in separate experiments using prion-infected mouse models that recapitulate the pathology seen in patients with CJD (10,41). We set out to determine if *in vitro* potency in the ScN2a-cl3 assay and PK parameters like AUC and the ratio of AUC/EC₅₀ predict *in vivo* efficacy in the models before testing in patients. Thus far, except for Compd B, no drug has been able to extend survival in these mouse models beyond 150 days (28), depending on the model. Mortality is typically observed at approximately 110–120 days post inoculation (dpi) with RML prions in wt FVB mice expressing normal levels of PrP^C (42).

From the first ~100 analogs of 2-AMTs, we evaluated 27 in single-dose PK studies (Table I). From these 27, we selected 10, based primarily on AUC and AUC/EC₅₀ ratios, and also C_{max} /EC₅₀ ratios, for multiple-dose PK studies, where we determined concentrations at the end of 3 days of dosing ($C_{3\text{-day}}$), AUC, and the ratio of AUC/EC₅₀ in brain and plasma. We also evaluated drug-like properties for 9 of the 2-AMTs, including solubility, permeability, and P-gp substrate potential, a good predictor of brain delivery limitations due to P-gp (Table II).

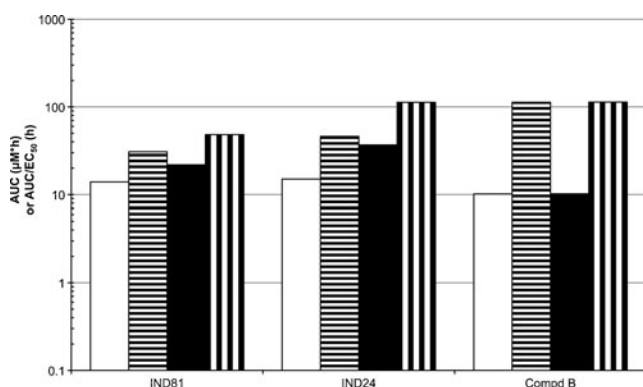


Fig. 9 AUC values for brain (black) and plasma (white) and AUC/EC₅₀ ratios for brain (vertical stripes) and plasma (horizontal stripes) based on brain and plasma concentrations and corrected for fraction unbound for IND81, IND24, and Compd B. Values are based on a dose of 210 mg/kg/day (IND81 and IND24) or 100 mg/kg/day (Compd B) given for 3 days. AUC values calculated from $C_{3\text{-day}} \times \tau$, as described in *Methods*.

IND24 and IND81 showed high AUC and AUC/EC₅₀ ratios in brain and plasma. Because they had some of the highest AUC and AUC/EC₅₀ ratios in brain and plasma after the 210 mg/kg/day dose, and acceptable drug-like properties, including toleration after 14 days of dosing at 210 mg/kg/day, they were selected to advance to *in vivo* animal studies. Some compounds, like IND85, actually had a better C_{max}/EC₅₀ ratio at either dose than IND24 and IND81, but had very low C_{3-day} concentrations, AUC, and AUC/EC₅₀ ratios in brain and plasma on multiple dosing and were not evaluated further.

From the C_{3-day} results, we reasoned that high AUC and AUC/EC₅₀ ratios greater than 10 would support a proof-of-concept experiment in prion-infected mice. Multiples of AUC/MIC ratios, where AUC is based on plasma data, have been associated with successful treatment and avoidance of resistance in the treatment of bacterial infections with many antibiotics (32, 33). Brain and plasma AUC and the AUC/EC₅₀ ratios were greater than 100 for IND24 and IND81 based on total drug concentrations (Fig. 8), and 113 for IND24 and 48 for IND81 based on unbound brain concentrations (Fig. 9). It was important to take into account the binding of the compounds in cell-culture media when using the EC₅₀ values for calculating the AUC/EC₅₀ ratios for unbound drug.

The “drug in liquid diet” approach used in the 3-day studies is practical because it simplifies drug administration during chronic dosing, allowing mice to achieve and maintain drug concentrations for long periods each day as mice are nocturnal and feed/drink predominantly during the dark cycle. It seemed crucial to have a dosing regimen that could be tolerated for up to 300 days or longer without the need to frequently handle mice daily over long periods of drug treatment.

It was important to characterize Compd B in PK studies to determine doses and formulations to be used as a positive control in studies in prion-infected mice. Compd B has been shown to extend the incubation times in prion-infected transgenic mice that overexpress PrP^C (28), but may not be acceptable for use in humans because it contains a hydrazone moiety that is metabolically unstable and is likely to lead to reactive intermediates with adverse side effects (34). Our studies with Compd B revealed lethal toxicity when administered chronically *in vivo* for 8 days at doses >110 mg/kg/day. We found that doses up to 100 mg/kg/day resulted in AUC/EC₅₀ ratios greater than 100 for total and unbound concentrations.

In summary, IND24 and IND81 reduced PrP^{Sc} in ScN2a-cl3 cells and have good PK properties *in vivo*, especially high AUC and AUC/EC₅₀ ratios in brain and plasma at doses of 210 mg/kg/day based on total and unbound compounds. We believe that these compounds are good candidates for testing in prion-infected mouse models.

ACKNOWLEDGMENTS AND DISCLOSURES

The authors thank Ms. Ana Serban, Ms. Julia Becker, and Mr. Frederic Letessier for D13 and D18 antibodies; Mr. Phillip Benner and the staff of the Hunter's Point animal facility for expert animal studies; Dr. Sina Ghaemmamghami for many helpful discussions; and Ms. Hang Nguyen for editorial assistance. This work was supported by grants from the National Institutes of Health (AG002132, AG010770, AG031220, and AG021601) as well as by gifts from the Sherman Fairchild Foundation, Rainwater Charitable Foundation, Lincy Foundation, Fight for Mike Homer Program, and Robert Galvin. MPJ is a consultant to Schrodinger LLC.

REFERENCES

1. Prusiner SB. Novel proteinaceous infectious particles cause scrapie. *Science*. 1982;216:136–44.
2. Weissmann C. Spongiform encephalopathies - the prion's progress. *Nature*. 1991;349:569–71.
3. Collinge J. Prion diseases of humans and animals: their causes and molecular basis. *Annu Rev Neurosci*. 2001;24:519–50.
4. Prusiner SB. Prions and neurodegenerative diseases. *N Engl J Med*. 1987;317:1571–81.
5. Hsiao K, Baker HF, Crow TJ, Poulter M, Owen F, Terwilliger JD, et al. Linkage of a prion protein missense variant to Gerstmann-Sträussler syndrome. *Nature*. 1989;338:342–5.
6. Alpers M, Gajdusek DC. Changing patterns of kuru: epidemiological changes in the period of increasing contact of the Fore people with western civilization. *Am J Trop Med Hyg*. 1965;14:852–79.
7. Prusiner SB. Shattuck lecture — neurodegenerative diseases and prions. *N Engl J Med*. 2001;344:1516–26.
8. Frost B, Diamond MI. Prion-like mechanisms in neurodegenerative diseases. *Nat Rev Neurosci*. 2010;11:155–9.
9. Caughey B, Baron GS, Chesebro B, Jeffrey M. Getting a grip on prions: oligomers, amyloids, and pathological membrane interactions. *Annu Rev Biochem*. 2009;78:177–204.
10. DeArmond SJ, McKinley MP, Barry RA, Braunfeld MB, McColloch JR, Prusiner SB. Identification of prion amyloid filaments in scrapie-infected brain. *Cell*. 1985;41:221–35.
11. Petkova AT, Leapman RD, Guo Z, Yau WM, Mattson MP, Tycko R. Self-propagating, molecular-level polymorphism in Alzheimer's beta-amyloid fibrils. *Science*. 2005;307:262–5.
12. Kordower JH, Chu Y, Hauser RA, Freeman TB, Olanow CW. Lewy body-like pathology in long-term embryonic nigral transplants in Parkinson's disease. *Nat Med*. 2008;14:504–6.
13. Desplats P, Lee HJ, Bae EJ, Patrick C, Rockenstein E, Crews L, et al. Inclusion formation and neuronal cell death through neuron-to-neuron transmission of alpha-synuclein. *Proc Natl Acad Sci USA*. 2009;106:13010–5.
14. Nekooki-Machida Y, Kurosawa M, Nukina N, Ito K, Oda T, Tanaka M. Distinct conformations of *in vitro* and *in vivo* amyloids of huntingtin-exon1 show different cytotoxicity. *Proc Natl Acad Sci USA*. 2009;106:9679–84.
15. Sydow A, Mandelkow EM. ‘Prion-Like’ propagation of mouse and human tau aggregates in an inducible mouse model of tauopathy. *Neurodegener Dis*. 2010;7:28–31.

16. Caughey B, Lansbury PT. Protofibrils, pores, fibrils, and neurodegeneration: separating the responsible protein aggregates from the innocent bystanders. *Annu Rev Neurosci.* 2003;26:267–98.
17. Novitskaya V, Bocharova OV, Bronstein I, Baskakov IV. Amyloid fibrils of mammalian prion protein are highly toxic to cultured cells and primary neurons. *J Biol Chem.* 2006;281:13828–36.
18. Race RE, Fadness LH, Chesebro B. Characterization of scrapie infection in mouse neuroblastoma cells. *J Gen Virol.* 1987;68:1391–9.
19. Kocisko DA, Baron GS, Rubenstein R, Chen J, Kuizon S, Caughey B. New inhibitors of scrapie-associated prion protein formation in a library of 2000 drugs and natural products. *J Virol.* 2003;77:10288–94.
20. Kocisko DA, Caughey B, Morrey JD, Race RE. Enhanced anti-scrapie effect using combination drug treatment. *Antimicrob Agents Chemother.* 2006;50:3447–9.
21. Trevitt CR, Collinge J. A systematic review of prion therapeutics in experimental models. *Brain.* 2006;129:2241–65.
22. Sim VL, Caughey B. Recent advances in prion chemotherapeutics. *Infect Disord Drug Targets.* 2009;9:81–91.
23. Korth C, May BCH, Cohen FE, Prusiner SB. Acridine and phenothiazine derivatives as pharmacotherapeutics for prion disease. *Proc Natl Acad Sci USA.* 2001;98:9836–41.
24. May BCH, Witkop J, Sherrill J, Anderson MO, Madrid PB, Zorn JA, *et al.* Structure-activity relationship study of 9-aminoacridine compounds in scrapie-infected neuroblastoma cells. *Bioorg Med Chem Lett.* 2006;16:4913–6.
25. Kempster S, Bate C, Williams A. Simvastatin treatment prolongs the survival of scrapie-infected mice. *NeuroReport.* 2007;18:479–82.
26. Kimata A, Nakagawa H, Ohyama R, Fukuuchi T, Ohta S, Doh-ura K, *et al.* New series of antiprion compounds: pyrazolone derivatives have the potent activity of inhibiting protease-resistant prion protein accumulation. *J Med Chem.* 2007;50:5053–6.
27. Thompson MJ, Borsenberger V, Louth JC, Judd KE, Chen B. Design, synthesis, and structure–activity relationship of indole-3-glyoxylamide libraries possessing highly potent activity in a cell line model of prion disease. *J Med Chem.* 2009;52:7503–11.
28. Kawasaki Y, Kawagoe K, Chen CJ, Teruya K, Sakasegawa Y, Doh-ura K. Orally administered amyloidophilic compound is effective in prolonging the incubation periods of animals cerebrally infected with prion diseases in a prion strain-dependent manner. *J Virol.* 2007;81:12889–98.
29. Supattapone S, Wille H, Uyechi L, Safar J, Tremblay P, Szoka FC, *et al.* Branched polyamines cure prion-infected neuroblastoma cells. *J Virol.* 2001;75:3453–61.
30. Ghaemmaghami S, May BCH, Renslo AR, Prusiner SB. Discovery of 2-aminothiazoles as potent antiprion compounds. *J Virol.* 2010;84:3408–12.
31. Gallardo-Godoy A, Gever J, Fife KL, Silber BM, Prusiner SB, Renslo AR. 2-Aminothiazoles as therapeutic leads for prion diseases. *J Med Chem.* 2011;54:1010–21.
32. Craig WA. The role of pharmacodynamics in effective treatment of community-acquired pathogens. *Johns Hopkins Adv Stud Med.* 2002;2:126–34.
33. Ambrose PG, Bhavnani SM, Rubino CM, Louie A, Gumbo T, Forrest A, *et al.* Pharmacokinetics-pharmacodynamics of antimicrobial therapy: it's not just for mice anymore. *Clin Infect Dis.* 2007;44:79–86.
34. Jonen HG, Werringtoner J, Prough RA, Estabrook RW. The reaction of phenylhydrazine with microsomal cytochrome P-450. Catalysis of heme modification. *J Biol Chem.* 1982;257:4404–11.
35. Ghaemmaghami S, Ullman J, Ahn M, St. Martin S, Prusiner SB. Chemical induction of misfolded prion protein conformers in cell culture. *J Biol Chem.* 2010;285:10415–23.
36. Obach RS. Prediction of human clearance of twenty-nine drugs from hepatic microsomal intrinsic clearance data: an examination of *in vitro* half-life approach and nonspecific binding to microsomes. *Drug Metab Dispos.* 1999;27:1350–9.
37. Hilgers AR, Conradi RA, Burton PS. Caco-2 cell monolayers as a model for drug transport across the intestinal mucosa. *Pharm Res.* 1990;7:902–10.
38. Kalvass JC, Maurer TS. Influence of nonspecific brain and plasma binding on CNS exposure: implications for rational drug discovery. *Biopharm Drug Dispos.* 2002;23:327–38.
39. Gibaldi M, Perrier D. *Pharmacokinetics.* 2nd ed. New York: Marcel Dekker, Inc; 1982.
40. Ha-Duong NT, Dijols S, Macherey AC, Goldstein JA, Dansette PM, Mansuy D. Ticlopidine as a selective mechanism-based inhibitor of human cytochrome P450 2C19. *Biochemistry.* 2001;40:12112–22.
41. Korth C, Kaneko K, Groth D, Heye N, Telling G, Mastrianni J, *et al.* Abbreviated incubation times for human prions in mice expressing a chimeric mouse–human prion protein transgene. *Proc Natl Acad Sci USA.* 2003;100:4784–9.
42. Ghaemmaghami S, Ahn M, Lessard P, Giles K, Legname G, DeArmond SJ, *et al.* Continuous quinacrine treatment results in the formation of drug-resistant prions. *PLoS Pathog.* 2009;5:e1000673.